Circulation

Cardiac Resident Macrophage-Derived Legumain Improves Cardiac Repair by Promoting Clearance and Degradation of Apoptotic Cardiomyocytes After Myocardial Infarction

Daile Jia, MD, PhD*; Siqin Chen, MD*; Peiyuan Bai(iD), MD*; Chentao Luo, MD*; Jin Liu, MD; Aijun Sun(iD), MD, PhD; Junbo Ge(iD), MD, PhD

BACKGROUND: Cardiac resident macrophages are self-maintaining and originate from embryonic hematopoiesis. After myocardial infarction, cardiac resident macrophages are responsible for the efficient clearance and degradation of apoptotic cardiomyocytes (efferocytosis). This process is required for inflammation resolution and tissue repair; however, the underlying molecular mechanisms remain unknown. Therefore, we aimed to identify the mechanisms of the continued clearance and degradation of phagolysosomal cargo by cardiac resident macrophages during myocardial infarction.

METHODS: Multiple transgenic mice such as Lgmn$^{-/-}$, Lgmn$^{F/F}$; LysM^{Cre}, Lgmn$^{F/F}$; Cx3cr1^{CreER}, Lgmn$^{F/F}$; Lyve^{Cre}, and cardiac macrophage Lgmn overexpression by adenovirus gene transfer were used to determine the functional significance of Lgmn in myocardial infarction. Immune cell filtration and inflammation were examined by flow cytometry and quantitative real-time polymerase chain reaction. Moreover, legumain (Lgmn) expression was analyzed by immunohistochemistry and quantitative real-time polymerase chain reaction in the cardiac tissues of patients with ischemic cardiomyopathy and healthy control subjects.

RESULTS: We identified *Lgmn* as a gene specifically expressed by cardiac resident macrophages. Lgmn deficiency resulted in a considerable exacerbation in cardiac function, accompanied by the accumulation of apoptotic cardiomyocytes and a reduced index of in vivo efferocytosis in the border area. It also led to decreased cytosolic calcium attributable to defective intracellular calcium mobilization. Furthermore, the formation of LC3-II–dependent phagosome around secondary-encountered apoptotic cardiomyocytes was disabled. In addition, Lgmn deficiency increased infiltration of MHC-II^{high} CCR2$^+$ macrophages and the enhanced recruitment of MHC-II^{low} CCR2$^+$ monocytes with downregulation of the anti-inflammatory mediators, interleukin-10, and transforming growth factor-β and upregulation of the proinflammatory mediators interleukin-1β, tumor necrosis factor-α, interleukin-6, and interferon-γ.

CONCLUSIONS: Our results directly link efferocytosis to wound healing in the heart and identify Lgmn as a significant link between acute inflammation resolution and organ function.

Key Words: macrophages ∎ myocardial infarction ∎ phagocytosis ∎ wound healing

---

Heart failure (HF) after myocardial infarction (MI) is a common cause of morbidity and mortality. Pharmacological advances in treatment through the use of angiotensin-converting enzyme inhibitors, angiotensin receptor/neprilysin inhibitors, β-blockers, and mineralocorticoid receptor antagonists have significantly reduced mortality; however, the residual risk of MI-induced HF remains increasingly high.[1] Therefore, novel

---

Clinical Perspective

What Is New?

- The expression of legumain (Lgmn) is increased in the patients with ischemic cardiomyopathy and in mouse models of ischemic injury.
- Lgmn deficiency in resident macrophages aggravates myocardial injury by promoting accumulation of apoptotic cardiomyocytes and reducing index of in vivo efferocytosis.
- Lgmn overexpression by use of an adenoviral vector in cardiac macrophages improves cardiac function in mice after myocardial infarction.

What Are the Clinical Implications?

- We clarified the mechanism of Lgmn-mediated efferocytosis in myocardial infarction, providing important insights into potential therapeutic targets for the prevention of cardiac ischemic injury.
- Selective overexpression of Lgmn in macrophages may be a novel therapeutic approach to prevent myocardial ischemic injury and cardiac remodeling.

Nonstandard Abbreviations and Acronyms

CCR2	C-C motif chemokine receptor 2
HF	heart failure
HLA-DR	human leukocyte antigen-DR isotype
KO	knockout
Lgmn	legumain
MHC-II	major histocompatibility complex II
MI	myocardial infarction
LV	left ventricular
PAR2	protease-activated receptor 2
TUNEL	terminal deoxynucleotidyl transferase-mediated dUTP-biotin nick-end labeling
WT	wild-type

and complementary approaches to preserve heart function are required.

During the acute inflammatory phase of MI, the amount of necrotic and apoptotic cardiomyocytes is a critical determinant of the severity of adverse remodeling that leads to HF.[2] The inefficient clearance of dying cardiomyocytes is also associated with suboptimal tissue remodeling after MI.[3,4] Therefore, strategies to efficiently clear dying cardiomyocytes may promote the resolution of inflammation and prevent extensive cell death, which may slow the progression to HF.

Efferocytosis is the processing and degradation of apoptotic cells through phagocytic endocytosis.[3,5] Although efficient efferocytosis activates anti-inflammatory pathways in the phagocyte, defective efferocy-

tosis leads to secondary postapoptotic cellular necrosis and expansion of tissue necrosis.[3,6] When a phagocyte engulfs a dying cardiomyocyte, it essentially doubles its cellular contents, yet phagocytes can sequentially ingest several apoptotic cardiomyocytes. In MI, when cardiomyocyte death is rampant, the high ratio of dying cardiomyocytes to phagocytes demands multiple, rapid uptake of dying cardiomyocyte by individual phagocytes and efficient clearance of the corpse-derived cellular material. However, the factors that influence this continued clearance and degradation of the phagolysosomal cargo remain unknown.

Multiple signaling events within professional phagocytes regulate processing and degradation of apoptotic cells to efficiently clear them and prevent the release of autoantigens. In the setting of a heterogeneous cardiac macrophage population, macrophage subsets have distinct origins and different repopulation mechanisms and functions.[5,7] The resident cardiac macrophages subset has been shown to efficiently take up dead cell cargo.[5] We performed bioinformatic analyses to identify candidate genes involved in endocytosis and intracellular trafficking. We identified legumain (*Lgmn*), which encodes an endolysosomal cysteine protease, as a potential candidate gene because of its specificity and high expression in cardiac MHC-II^{low} CCR2$^-$ and TIMD4$^+$ CCR2$^-$ macrophages. Furthermore, we have investigated the link between LGMN deficiency and the ability of resident cardiac macrophages to clear apoptotic cardiomyocytes using a murine model of MI and have demonstrated that macrophage-derived LGMN is specifically required for the clearance and degradation of dying adult cardiomyocytes. In addition, LGMN modulation may offer therapeutic benefit for the treatment of MI.

METHODS

The data, analytical methods, and study materials are available from the corresponding author on reasonable request.

An expanded Methods section is available in the Supplemental Material.

Mice

Wild-type (WT) C57BL6/J mice (male, 8–10 weeks old; SLRC Laboratory Animal, Shanghai, China) were used in this study. Lgmn$^{F/F}$ mice, possessing 2 loxP sites flanking exon 3 of the Lgmn gene (constructed by Shanghai Biomodel Organism, Shanghai, China), were maintained in a C57BL/6 genetic background. Lgmn$^{-/-}$ mice were generated by crossing Lgmn$^{F/F}$ mice with C57BL/6 DDX4-Cre mice (Shanghai Biomodel Organism). Lgmn$^{F/F}$ mice were crossed with C57BL/6 LysM^{Cre} mice to generate Lgmn$^{F/F}$×LysM^{Cre} mice. Cx3cr1^{creER} mice and Lyve$^{cre/GFP}$ mice were obtained from The Jackson Laboratory (Bar Harbor, ME). Lgmn$^{F/F}$ mice were crossed with Cx3cr1^{creER} mice and Lyve$^{cre/GFP}$ mice to generate Lgmn$^{F/F}$×Cx3cr1^{creER} and Lgmn$^{F/F}$×Lyve$^{cre/GFP}$ mice. Fluorescent protein expression in cardiomyocytes was induced by crossing α-MHC^{Cre}

with Rosa26-tdTomato. This study and all animal procedures conformed to the Guide for the Care and Use of Laboratory Animals, published by the National Institutes of Health (NIH publication No. 85-23, revised 1996) and were approved by the animal care and use committee of Fudan University (SYXK2016-0006).

Human Left Ventricular Tissues

All procedures performed in studies involving human participants were in accordance with the ethics standards of the institutional or national research committee and with the 1964 Declaration of Helsinki and its later amendments or comparable ethics standards. This study was approved by the Zhongshan Hospital, Fudan University, Review Board (B2020-163R). To study human ischemic HF, we obtained human left ventricular (LV) samples from explanted hearts at the time of transplantation. Subjects were grouped as controls (noncardiac cause of death, including car accident or trauma) or with ischemic cardiomyopathy, and patients receiving either chemotherapy or radiation were excluded. The collected tissues were subjected to HIV/hepatitis B testing before use and were treated as potentially contagious for blood-borne pathogens.

Statistical Analysis

Results are presented as mean± SEM. Data normality was determined by the Shapiro-Wilk test. Comparisons between 2 groups were made with the Student t test, whereas the data obtained from multiple groups were compared by use of 1-way, 2-way, and 2-way repeated-measures ANOVA followed by Bonferroni post hoc analysis. Nonnormal data were analyzed by Mann-Whitney U test or Kruskal-Wallis test with Dunn multiple comparisons. Specific statistical tests and results for each panel are described in Table S7. A value of $P<0.05$ was considered significant. GraphPad Prism 5.0 (GraphPad Prism Software Inc, San Diego, CA) and SPSS 15.0 for Windows (SPSS, Inc, Chicago, IL) were used for statistical analysis.

## RESULTS

Lgmn Expression Increases After MI in Mice

To identify putative genes involved in endocytosis and intracellular trafficking, we compared the transcriptomic signatures of macrophages isolated at different time points from the hearts of mice after MI surgery.[8] We found that 11 genes were upregulated in the early phase after MI, suggesting that the expression of these genes is induced during efferocytosis (Figure S1A). After screening the expression profiles of these 11 genes in the Immgen and bioGPS databases, we identified Lgmn as a potential candidate gene because of its high and specific expression in macrophages (Figure S1B and S1C). To elucidate the involvement of Lgmn in MI, we first investigated its spatiotemporal expression in mouse myocardial tissues. Lgmn mRNA and protein expression levels were shown to increase significantly on day 5 in infarct area and border area compared with baseline levels, whereas the expressions remained low and unchanged

after infarction in the noninfarcted area (Figure 1A and 1B). Double-immunofluorescence staining for Lgmn along with CD68, Ly-6G, or CD3 staining confirmed that Lgmn was expressed predominately by cardiac CD68+ macrophages, but not Ly-6G+ neutrophils or CD3+ T cells, after MI (Figure 1C).

Cardiac macrophages can be divided into 3 distinct subsets that are based on the expression of major histocompatibility complex II (MHC-II) and C-C motif chemokine receptor 2 (CCR2): MHC-II^{low} CCR2−, MHC-II^{high} CCR2−, and MHC-II^{high} CCR2+ macrophages (Figure 1D). Using cells sorted by fluorescence-activated cell sorter from the ischemic zones (infarct area and border area) 5 days after MI, we showed that Lgmn mRNA was expressed predominately in MHC-II^{low} CCR2− macrophages rather than in MHC-II^{high} CCR2− macrophages or MHC-II^{high} CCR2+ macrophages (Figure 1E). However, control cardiac macrophage subsets expressed similar and low levels of Lgmn (Figure 1E). Immunofluorescence staining also showed that Lgmn was not colocalized with MHC-II or CCR2 in mouse hearts on day 5 after MI (Figure 1F). Specifically in the myocardium, TIMD4 can be used to identify resident macrophages after MI.[7] We sorted TIMD4+ CCR2− resident macrophages, TIMD4− CCR2− macrophages, and TIMD4− CCR2+ macrophages from the ischemic zones 5 days after MI and demonstrated that Lgmn mRNA was expressed mainly in TIMD4+ CCR2− resident macrophages rather than in TIMD4− CCR2− macrophages or TIMD4− CCR2+ macrophages after MI (Figure 1G and 1H).

Lgmn Expression Increases in Ischemic Cardiomyopathy

We evaluated 3 subsets of human cardiac macrophages that were grouped according to MHC-II class isotype human leukocyte antigen-DR isotype (HLA-DR) and CCR2 expression: HLA-DR^{high} CCR2−, HLA-DR^{high} CCR2+, and HLA-DR^{low} CCR2+ (Figure 2A). To identify putative genes involved in endocytosis and intracellular trafficking, we compared the transcriptomic signatures of these macrophage subsets in ischemic cardiomyopathies.[9] We identified LGMN as a potential candidate gene because it had the highest expression compared with 12 other genes, and its expression was specific to HLA-DR^{high} CCR2− cardiac resident macrophages (Figure S2A–S2C). Moreover, the LGMN mRNA and protein expression levels were significantly higher in the cardiac tissues of patients with ischemic cardiomyopathy compared with those of healthy control subjects (Figure 2B and 2C). Further analyses revealed that Lgmn was expressed mainly in HLA-DR^{high} CCR2− macrophages (Figure 2D). Next, we sorted cardiac macrophages from patients with ischemic cardiomyopathies. Similar to our transcriptomic analysis, we found that Lgmn mRNA was specifically expressed in HLA-DR^{high} CCR2− macrophages but not in
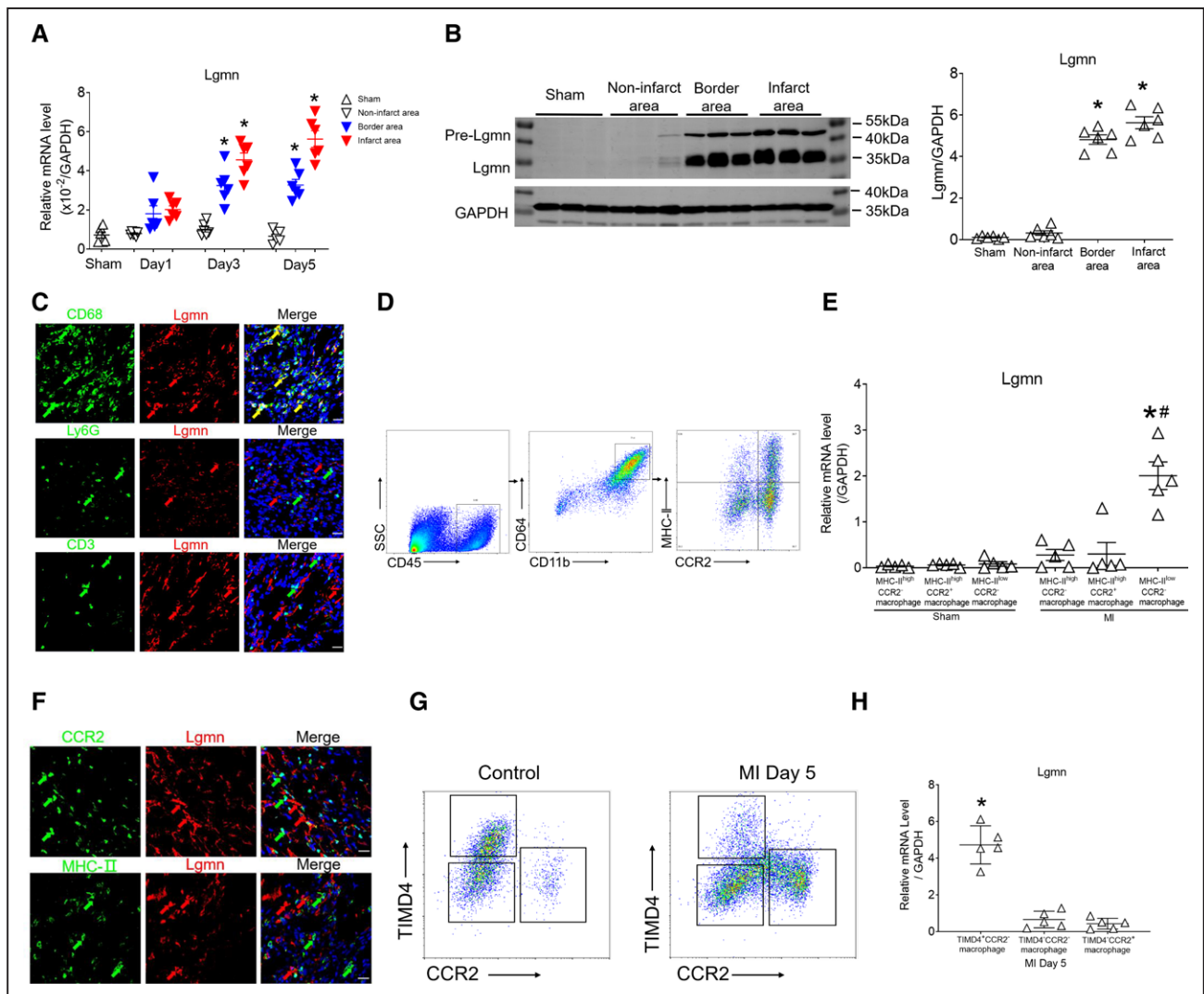
**Figure 1. Lgmn is increased in the heart after MI.**

A, Legumain (Lgmn) expression levels in noninfarcted area, border area, and infarct area were analyzed at different time points after myocardial infarction (MI; n =6; *P<0.05 vs noninfarcted area by 1-way ANOVA followed by Bonferroni post hoc analysis). **B**, Lgmn protein levels in noninfarcted area, border area, and infarct area were determined at day 5 after MI (n=6; *P<0.05 vs noninfarcted area by 1-way ANOVA followed by Bonferroni post hoc analysis). **C**, Representative immunostaining of Lgmn (red), CD68 (green), Ly6G (green), CD3 (green), and nuclei (4′,6-diamidino-2-phenylindole; blue) in murine hearts on day 5 after MI. Scale bar, 50 μm. Red arrows indicates Lgmn+ cells; green arrows, CD68+, Ly6G+, or CD3+ cells; and yellow arrows, CD68+/ Lgmn+ cells. **D**, Gating strategy for cardiac macrophages from ischemic zones (infarct area and border area). **E**, Lgmn expression levels were analyzed in MHC-II^{low} CCR2$^-$ macrophages, MHC-II^{high} CCR2$^-$ macrophages, and MHC-II^{high} CCR2$^+$ macrophages isolated from hearts on day 5 after MI (n=5; *P<0.05 vs MHC-II^{high} CCR2$^-$ macrophages and MHC-II^{high} CCR2$^+$ macrophages MI group; #P<0.05 vs sham by 2-way ANOVA followed by Bonferroni post hoc analysis). **F**, Representative immunostaining of Lgmn (red), C-C motif chemokine receptor 2 (CCR2; green), major histocompatibility complex II (MHC-II; green), and nuclei (4′,6-diamidino-2-phenylindole; blue). Scale bar, 50 μm. Red arrows indicate Lgmn+ cells; and green arrows, CCR2+ or MHC-II + cells. **G**, Gating strategy for cardiac macrophages from ischemic zones (infarct area and border area). **H**, Lgmn expression levels were analyzed in Timd4+ CCR2$^-$ resident macrophages, Timd4$^-$ CCR2$^-$ macrophages, and Timd4$^-$ CCR2$^+$ macrophages isolated from hearts on day 5 after MI (n=5; *P<0.05 vs Timd4$^-$ CCR2$^-$ macrophages and Timd4$^-$ CCR2$^+$ macrophages by 1-way ANOVA followed by Bonferroni post hoc analysis). See Table S7 for statistical details.

HLA-DR^{high} CCR2$^+$ macrophages or HLA-DR^{low} CCR2$^+$ monocytes (Figure 2E).

LGMN Deficiency Exacerbates MI

To investigated the effects of Lgmn deficiency in MI, we compared the severity of MI between *Lgmn* knockout (KO) and WT C57BL/6 mice. Echocardiography was

used to confirm the absence of any preexisting cardiac abnormalities in the *Lgmn* KO mice before MI surgery, and the echocardiographic parameters of the *Lgmn* KO mice were comparable to those of the WT mice (Table S2). Both the *Lgmn* KO and WT mice were then subjected to MI, and cardiac function was analyzed on days 7 and 14 after MI (Figure 3A). The echocardiographic analyses revealed expansion of LV dilatation (LV end-diastolic
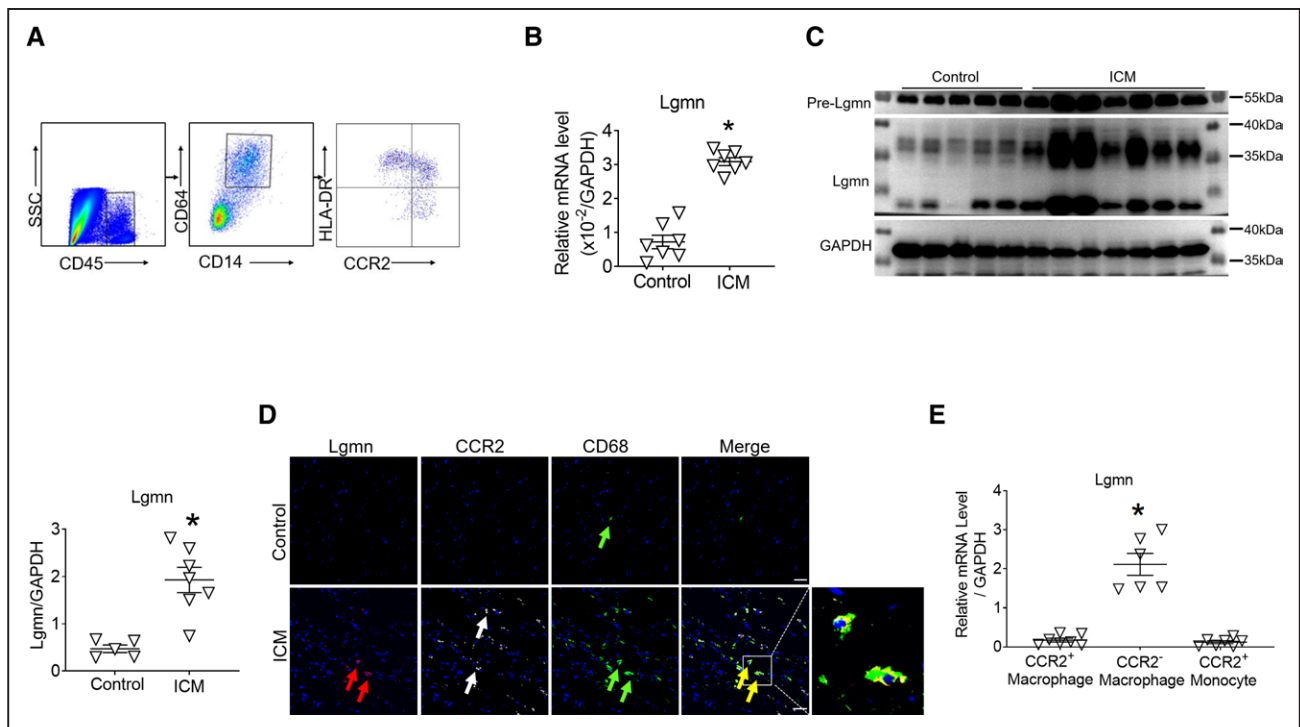
Figure 2. Lgmn expression increases in ICM.

A, Flow cytometry gating scheme used to identify and characterize cardiac macrophage populations. **B**, Legumain (Lgmn) expression levels were analyzed in ischemic cardiomyopathy (ICM) and control healthy tissues (n=7; *$P<0.05$ vs control group by Student t test). **C**, Lgmn protein levels were determined in ICM and control healthy heart tissues (n=5–7; *$P<0.05$ vs control group by Student t test). **D**, Representative immunostaining of Lgmn (red), C-C motif chemokine receptor 2 (CCR2; gray), CD68 (green), and nuclei (4′,6-diamidino-2-phenylindole; blue) in ICM and control healthy tissues. Scale bar, 50 µm. Green arrows indicate CD68+ cells; red arrows, Lgmn+ cells; and yellow arrows, CD68+/Lgmn+ cells. **E**, Lgmn expression levels were analyzed in HLA-DRhigh CCR2− macrophages, HLA-DRhigh CCR2+ macrophages, and HLA-DRlow CCR2+ monocytes isolated from hearts of patients with ICM (n=6; *$P<0.05$ by 1-way ANOVA followed by Bonferroni post hoc analysis). See Table S7 for statistical details.

diameter) and reduction in fractional shortening in the *Lgmn* KO mice compared with WT mice (Figure 3A). Furthermore, *Lgmn* KO mice exhibited increased heart and lung weight to body weight ratios on day 14 after MI compared with WT mice, indicating their compromised cardiac function (Table S2). Next, we constructed myeloid LGMN-depleted mice by crossing *Lgmn*F/F mice with LysMCre mice (*Lgmn*F/F×LysMCre mice) to investigate whether myeloid-specific LGMN deficiency also exacerbated the pathogenic alterations of MI. These mice exhibited significant decreases in fractional shortening and increases in LV end-diastolic volume and LV end-systolic volume at days 7 and 14 after MI, indicating deteriorated cardiac function (Figure 3B and Table S3).

LGMN Deficiency Augments Accumulation of Apoptotic Cardiomyocytes

We used immunohistochemical staining to analyze myocardial wound-healing parameters. The expression levels of α-smooth muscle actin, collagen I, and collagen III were not significantly altered in *Lgmn* KO mice on both days 7 and 14 after MI compared with WT mice (Figure S3A and S3B). Next, myocardial angiogenesis was analyzed by CD31 staining at days 5 and 14 after

MI because of its important role in cardiac remodeling and wound healing. Both quantitative polymerase chain reaction and immunostaining demonstrated that CD31 expression was not significantly altered in the *Lgmn* KO mice on days 7 and 14 after MI compared with WT mice (Figure S3C and S3D).

Furthermore, terminal deoxynucleotidyl transferase-mediated dUTP-biotin nick-end labeling (TUNEL) staining was performed to detect cardiomyocyte apoptosis on day 14 after MI in the border area. The rate of TUNEL-positive cardiomyocytes was significantly higher in *Lgmn* KO mice after MI than in WT mice (Figure 4A and 4B). Moreover, the *Lgmn* KO mice also displayed elevated levels of the proapoptotic molecules, BAX, and cleaved caspase-3 after MI compared with the WT mice (Figure 4C and 4D). Numerous reports have linked cardiomyocyte apoptosis to post-MI cardiac repair; however, studies on the fate of the cardiomyocytes after their death are comparatively lacking. Next, as a surrogate indicator for in vivo efferocytosis, we examined macrophage and cardiomyocyte colocalization in myocardial tissue sections from the *Lgmn* KO and WT mice using cardiomyocyte marker cardiac troponin I and macrophage marker CD68. We then calculated the percentage of cardiomyocyte-containing macrophages to determine
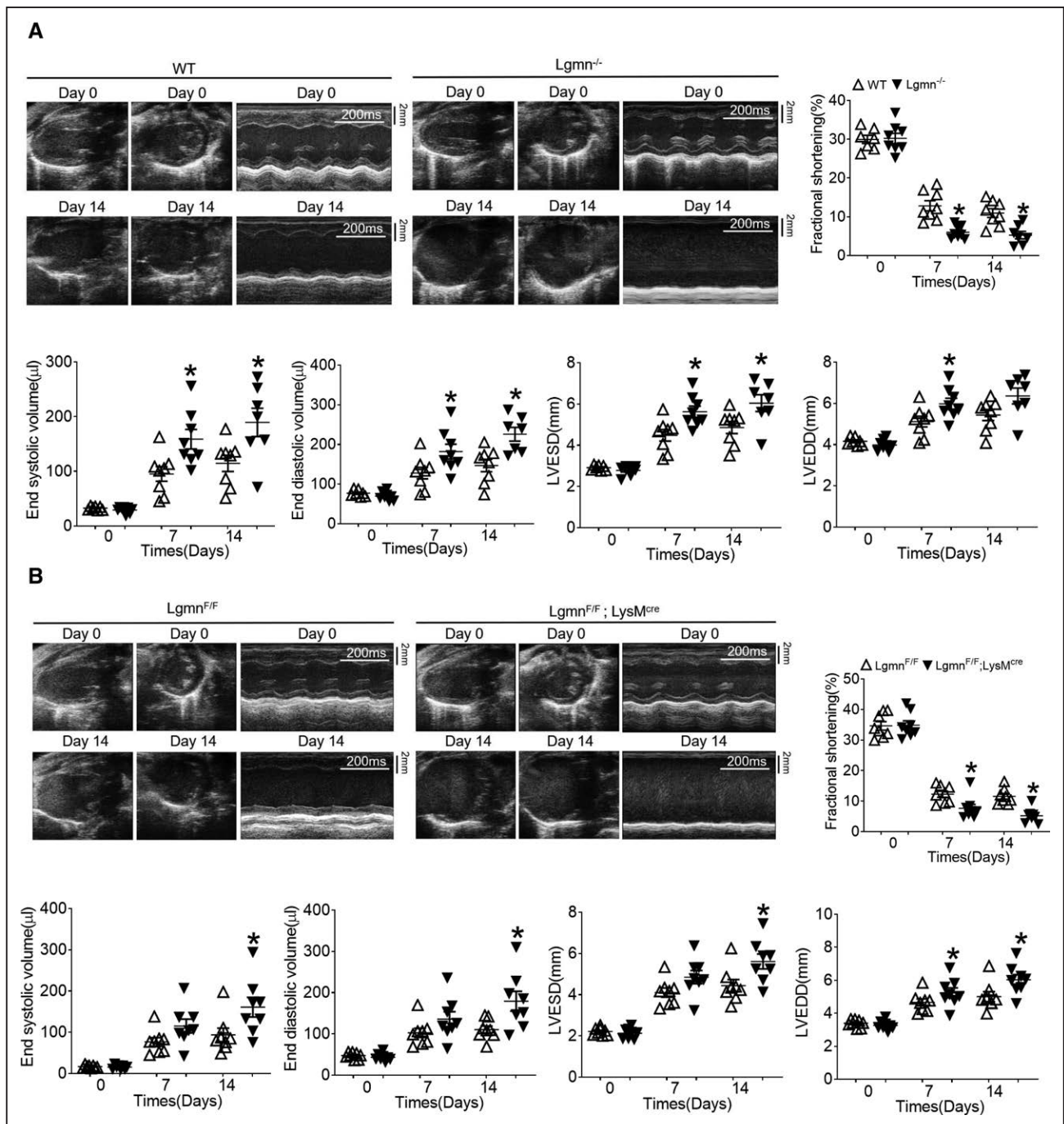
Figure 3. Cardiac function comparison between WT, *Lgmn*⁻/⁻, *Lgmn*^F/F, and *Lgmn*^F/F×LysM^Cre mice after MI.
A, Representative parasternal long-axis views, short-axis views, and M-mode images. Echocardiographic analysis of left ventricular end-systolic volume (LVESV), left ventricular end-diastolic volume (LVEDV), fractional shortening (FS), left ventricular end-systolic diameter (LVESD), and left ventricular end-diastolic diameter (LVEDD) on days 0, 7, and 14 after the myocardial infarction (MI) or sham operation in wild-type (WT) and Lgmn⁻/⁻ mice (n=7–8). **B**, Echocardiographic analysis of LVESV, LVEDV, FS, LVESD, and LVEDD on days 0, 7, and 14 after the MI or sham operation in Lgmn^F/F and Lgmn^F/F×LysM^Cre mice (n=8). Data are expressed as mean±SEM. *P<0.05 vs WT or Lgmn^F/F MI, respectively. Data in **A** and **B** were analyzed with 2-way repeated-measures ANOVA. See Table S7 for statistical details. Lgmn indicates legumain.

whether LGMN deficiency augmented the accumulation of apoptotic cardiomyocytes in vivo. (Figure 4E). However, the percentage of these cardiomyocyte-containing macrophages was significantly decreased in the myocardial tissues from the *Lgmn* KO mice at day 5 after MI (Figure 4F). To definitively test for the internaliza-

tion of cardiomyocyte-derived proteins by macrophages and the effect of LGMN deficiency, flow cytometry was used to isolate macrophages from the cardiac tissues of CCR2^GFP; α-MHC-Cre; R26-tdTomato and *Lgmn* KO; CCR2^GFP; α-MHC-Cre; R26-tdTomato mice after MI. These results further confirmed impaired efferocytosis in
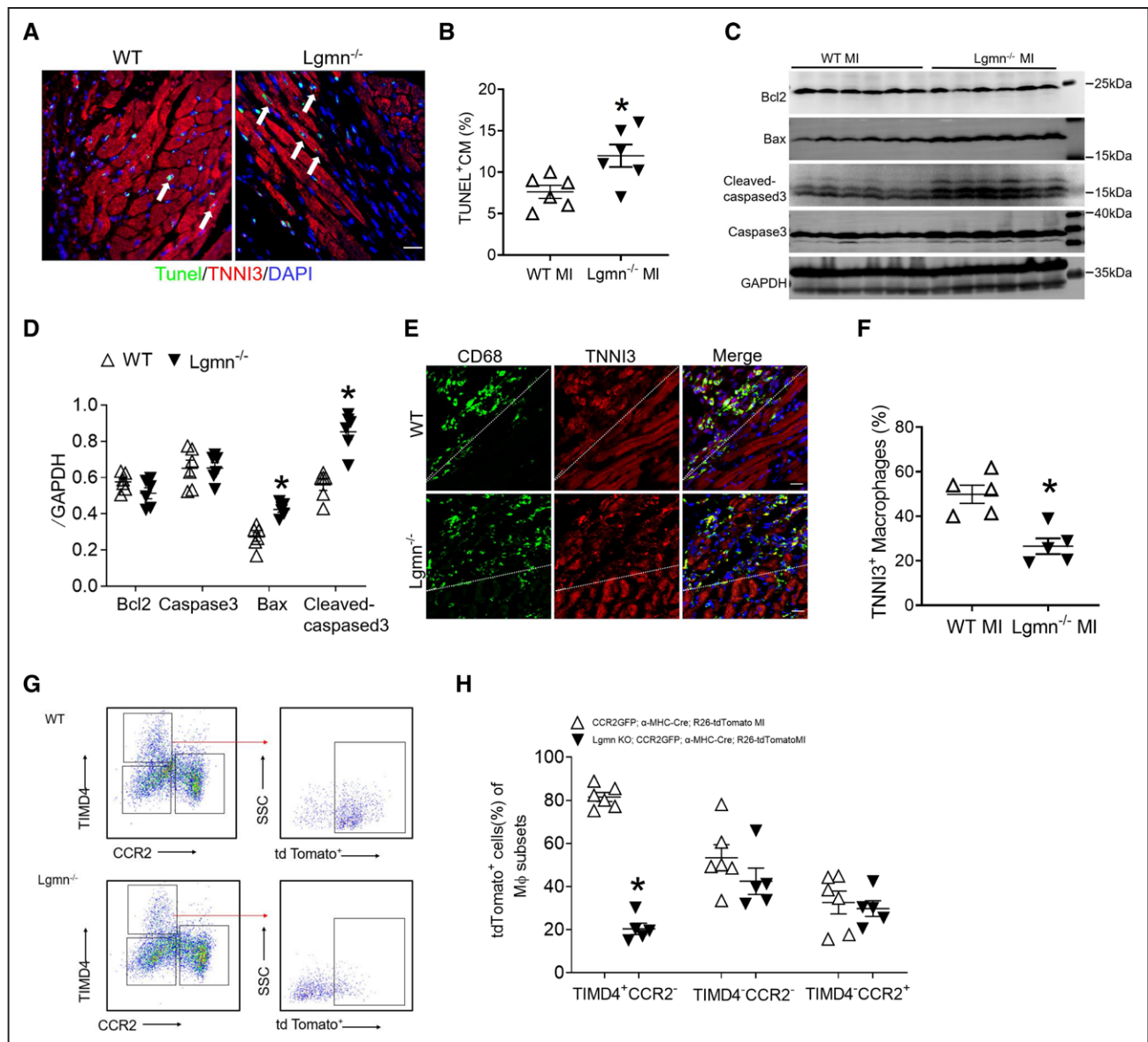
Figure 4. LGMN deficiency leads to increased accumulation of apoptotic cardiomyocytes.
A, Representative photomicrographs of terminal deoxynucleotidyl transferase dUTP nick-end labeling (TUNEL) and nuclear DAPI staining of cardiomyocyte marker cardiac troponin I (TNNI3)–positive cardiomyocytes obtained from wild-type (WT) and Lgmn$^{-/-}$ mice on day 5 after myocardial infarction (MI). White arrows point out TUNEL-positive (green) cardiomyocyte (red) nuclei (blue; scale bar, 20 μm). **B**, Percentage of TUNEL-positive cardiomyocytes after MI, compared between WT and Lgmn$^{-/-}$ mice (n=6; *P<0.05 vs WT MI by Student t test). **C** and **D**, Representative Western blot analyses and summary data showing the protein expression of Bcl-2, Bax, cleaved caspase-3, and caspase-3 in WT and Lgmn$^{-/-}$ mice on day 5 after MI (n=6; *P<0.05 vs WT MI by Student t test). **E**, Immunohistochemistry shows colocalization of CD68$^+$ macrophages with TNNI3$^+$ cardiomyocytes (yellow). Scale bar, 20 μm. **F**, Analysis of internalization of cardiomyocyte-derived proteins in macrophages. Macrophages that stain positive for cardiomyocyte TNNI3 are scored as having internalized cardiomyocyte-derived proteins (n=5; *P<0.05 vs WT MI by Mann-Whitney U test). **G**, Flow cytometry gating scheme used to identify and characterize TIMD4$^+$ CCR2$^-$ cardiac macrophage internalizing cardiomyocyte-derived proteins. **H**, Analysis of TIMD4$^+$ CCR2$^-$, TIMD4$^-$ CCR2$^-$, and TIMD4$^-$ CCR2$^+$ cardiac macrophage internalizing cardiomyocyte-derived proteins (n=5–6; *P<0.05 vs CCR2^{GFP}; α-MHC-Cre; R26-tdTomato by Mann-Whitney U test). See Table S7 for statistical details. CCR2 indicates C-C motif chemokine receptor 2; and Lgmn, legumain.

response to LGMN deficiency because fewer TIMD4$^+$ CCR2$^-$ macrophages containing the internalized tdTomato$^+$ signal were isolated from the *Lgmn* KO; CCR2^{GFP}; α-MHC-Cre; R26-tdTomato mice than the CCR2^{GFP}; α-MHC-Cre; R26-tdTomato control mice (Figure 4G and 4H). In addition, the percentage of TIMD4$^-$ CCR2$^-$ macrophages and TIMD4$^-$ CCR2$^+$ macrophages expressing

the internalized tdTomato$^+$ signal was similar between WT and *Lgmn* KO mice (Figure 4H).

LGMN Deficiency Increases Infarction Size

The extent of myocardial apoptosis is associated with the degree of myocardial necrosis or infarction size, and

infarction size is a major determinant of patient prognosis.[10] We next examined whether impaired efferocytosis of apoptotic cardiomyocytes contributed to larger infarction sizes in the *Lgmn* KO mice. Masson trichrome staining revealed no morphological differences in the sham-operated hearts of the *Lgmn* KO and WT mice (Figure S4A). In contrast, the *Lgmn* KO mice displayed larger infarction sizes at day 14 after MI than the WT mice (Figure S4A and S4B). Moreover, infarctions were significantly larger in the *Lgmn*[F/F]×LysM[Cre] mice than the *Lgmn*[F/F] mice (Figure S4C and S4D).

Lgmn Is Required for the Clearance of Apoptotic Cardiomyocytes

Efferocytosis involves recognition of apoptotic cells by cell receptors and then phagocytosis and phagolysosomal digestion of the apoptotic cells.[11] RNA sequencing of cardiac macrophages and protein analysis of infarct tissue from *Lgmn*-KO and WT mice after MI revealed that Lgmn deficiency had no overt influence on cell receptors involved in recognition of apoptotic cells such as CD36, LRP1/CD91, BAI1, TIM4, and MerTK (Figure S5). Thus, we focused on phagocytosis and phagolysosomal digestion of the apoptotic cells. To directly test the role of Lgmn in engulfment, we cocultured dying primary adult mouse cardiomyocytes with MHC-II[low] CCR2^{−} resident cardiac macrophages. We observed 2 key phenotypes in the *Lgmn* KO (*Lgmn*^{−/−}) macrophages. First, these macrophages exhibited impaired high-burden efferocytosis. At relatively early time points or low cardiomyocyte-to-macrophage ratios, the *Lgmn*^{−/−} macrophages displayed cardiomyocyte association similar to that of the control macrophages; however, this decreased at longer time points or higher cardiomyocyte-to-macrophage ratios (Figure 5A and 5B). These results were confirmed by microscopy-based measurement using CypHer5E-labeled cardiomyocyte-derived material, which become fluorescent in acidic phagolysosomes (Figure 5C). From these data, we hypothesized that LGMN enabled high-burden efferocytosis in macrophages by facilitating the internalization of multiple cardiomyocyte-derived material. To test this hypothesis, we conducted a 2-stage efferocytosis experiment. Macrophages were first incubated for 45 minutes with calcein AM-labeled cardiomyocyte-derived material. Then, the cardiomyocyte-derived materials were removed, and the macrophages were allowed a 120-minute rest interval before being incubated with R26-tdTomato−labeled cardiomyocyte-derived material. As expected, a smaller percentage of the *Lgmn*^{−/−} macrophages had internalized both labels compared with the control macrophages (Figure 5D). Second, the *Lgmn*^{−/−} macrophages exhibited a reduced phagocytic capacity because less apoptotic material was engulfed and properly processed by these macrophages. We observed less fragmentation of the labeled dying cardiomyocyte-

derived material in the *Lgmn*^{−/−} macrophages that successfully internalized cardiomyocyte-derived material compared with the control macrophages, suggesting defective degradation of their phagolysosomal cargo. To quantify phagolysosomal cargo degradation, we incubated *Lgmn*^{−/−} and control macrophages for 45 minutes with R26-tdTomato−labeled cardiomyocyte-derived material. After removal of any unengulfed cardiomyocyte-derived material, the percentage of macrophages displaying nonfragmented R26-tdTomato labeling was determined over a 3-hour period. As expected, a larger percentage of the *Lgmn*^{−/−} macrophages contained nonfragmented cardiomyocyte-derived material compared with the control macrophages (Figure 5E).

Lgmn-Deficient Macrophages Exhibit Defective LC3-II−Associated Phagocytic Degradation

The *Lgmn*^{−/−} macrophages exhibited less fragmentation of the internalized cardiomyocyte-derived material compared with the control macrophages, indicating defective degradation of their phagolysosomal cargo. Therefore, we investigated whether this observation was attributable to defective LC3-associated phagocytosis, the process of LC3-II and phagosome conjugation that enables phagosome-lysosome fusion and cardiomyocyte degradation.[12,13] We found that LGMN deficiency led to the downregulation of LC3-II in the hearts of the *Lgmn* KO mice after MI compared with the WT mice (Figure 5F). Moreover, *Lgmn*^{−/−} and control macrophages were incubated with R26-tdTomato−labeled cardiomyocyte-derived material for 1 hour. Then, the unengulfed cardiomyocyte-derived material was removed, and the macrophages were fixed, treated with digitonin to remove nonmembrane-bound LC3, and immunostained for LC3. Fluorescence microscopic imaging confirmed the presence of LC3 in the cardiomyocyte-containing control macrophages, whereas markedly less LC3 was detected in the cardiomyocyte-containing *Lgmn*^{−/−} macrophages (Figure 5G).

Defective Phagocytic Sealing and Degradation in Lgmn-Deficient Resident Cardiac Macrophages Are Linked to Decreased Cytosolic Calcium

To explore how LGMN deficiency may be linked to defective efferocytosis, we first investigated the role of cytoplasmic calcium because increased macrophage cytosolic calcium is required for efficient apoptotic cell clearance[14,15] and cytosolic calcium decreases in response to defective intracellular calcium mobilization in certain settings.[16] We hypothesized that LGMN deficiency may impair the apoptotic cell-induced increase in macrophage cytosolic calcium through the defective cleavage of protease-activated receptor 2 (PAR2),[16] thus leading to defective
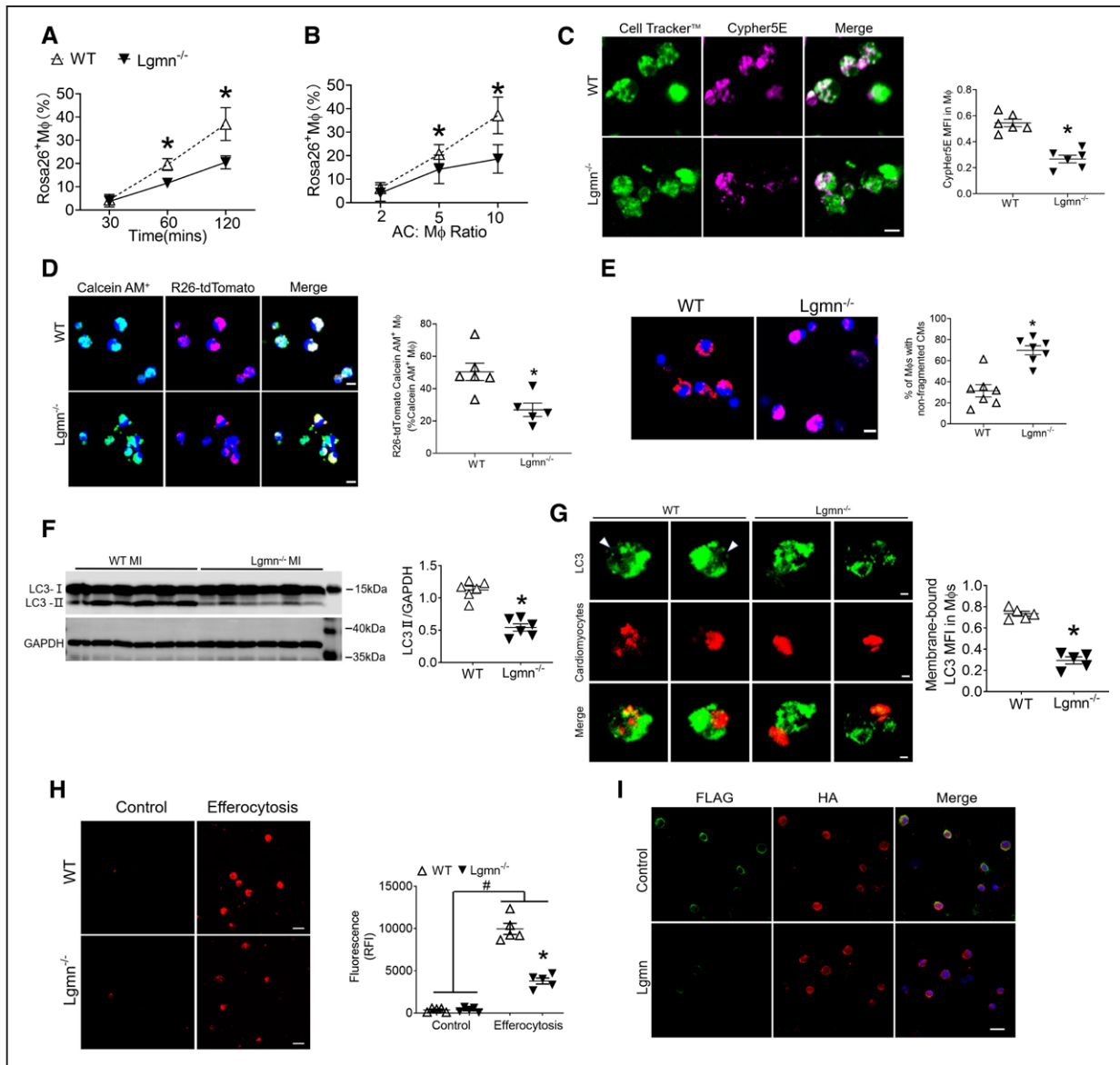
Figure 5. Lgmn-deficient macrophages have a defect in apoptotic cardiomyocytes degradation.
A and **B**, Control or legumain (*Lgmn*) knockout (KO) resident cardiac macrophages were incubated with R26-tdTomato+ cardiomyocytes at various times at a 10:1 cardiomyocyte:macrophage ratio or at various ratios for 1 hour (AC:Mφ= apoptotic cardiomyocytes : macrophages). Efferocytosis was quantified as the total percentage of macrophages positive for R26-tdTomato+ cardiomyocytes(n=6; *$P<0.05$ by 2-way ANOVA followed by Bonferroni post hoc analysis). **C**, CypHer5E-labeled apoptotic cardiomyocytes were incubated with macrophages at a 10:1 ratio for 45 minutes. The unengulfed apoptotic cardiomyocytes were removed by rinsing, and efferocytosis was analyzed by confocal fluorescence microscopy for CypHer5E mean fluorescence intensity (MFI) in macrophages (n=6; *$P<0.05$ vs WT by Mann-Whitney *U* test). **D**, Control or Lgmn KO macrophages were incubated with calcein AM-labeled cardiomyocytes at a 5:1 cardiomyocyte:macrophage ratio for 45 minutes. Cardiomyocytes were removed and rested for 120 minutes, before macrophages were incubated with R26-tdTomato cardiomyocytes at a 5:1 ratio for 45 minutes. Unengulfed cardiomyocytes were removed, and the percentage of calcein AM+ R26-tdTomato+ macrophages among calcein AM+ macrophages was analyzed by immunofluorescence (n=5–6; *$P<0.05$ vs WT by Mann-Whitney *U* test). **E**, Control or *Lgmn* KO macrophages were incubated for 45 minutes with R26-tdTomato cardiomyocytes. Unengulfed cardiomyocytes were removed, and macrophages were incubated for 3 hours. Cells were fixed with 2% formaldehyde, and cardiomyocyte fragmentation was quantified as the percentage of macrophages with fragmented R26-tdTomato fluorescence (n =7; *$P<0.05$ vs WT by Student *t* test). Scale bar, 20 mm. **F**, Western blot analysis of LC3-I and LC3-II expression in WT and Lgmn−/− mice after MI (n=6; *$P<0.05$ vs WT by Student *t* test). **G**, Control and *Lgmn*-deficient macrophages were incubated with R26-tdTomato cardiomyocytes (red) for 45 minutes, fixed in 4% formaldehyde for 15 minutes, incubated with 50 mg/mL digitonin for 5 minutes, and immunostained for LC3 (green). Arrowheads in control images depict a ring of immunostained LC3 surrounding an apoptotic cardiomyocyte-containing phagosome (not seen in Lgmn-deficient macrophage images). Cells were analyzed by confocal fluorescence microscopy for membrane-bound LC3 MFI in apoptotic cardiomyocyte+ macrophages (n=5; *$P<0.05$ vs WT by Mann-Whitney *U* test). **H**, Representative images of fluo-3 fluorescence (green) in mouse cardiac macrophages and quantification of fluorescence intensities (n=5; *$P<0.05$ vs efferocytosis WT; #$P<0.05$ vs control by 2-way ANOVA followed by Bonferroni post hoc analysis). **I**, Localization of protease-activated receptor 2 (PAR2) with antibodies against extracellular N-terminal FLAG and intracellular C-terminal HA epitopes (inset) in macrophage-FLAG-PAR2-HA cells incubated with vehicle (control), Lgmn, or trypsin. Arrows denote plasma membrane localization; arrowheads denote endosomal localization. Scale bar, 20 µm. See Table S7 for statistical details.

efferocytosis. We first determined whether the $Lgmn^{-/-}$ macrophages exhibited altered cytosolic calcium levels after exposure to apoptotic cardiomyocytes. The mobilization of intracellular calcium was significantly compromised in the $Lgmn^{-/-}$ macrophages after engulfing apoptotic cardiomyocyte-derived material (Figure 5H). The increase in cytosolic calcium is mediated through the cleavage of PAR2 by LGMN.[16] PAR2 expressing an extracellular FLAG epitope and intracellular HA epitope (FLAG-PAR2-HA) was used to confirm the cleavage of intact PAR2 by LGMN at the plasma membrane in $Lgmn^{-/-}$ macrophages (Figure 5H). These macrophages were incubated with LGMN (100 nmol/L, Hanks Balanced Salt Solution, pH 5.0) or vehicle (buffer control), and then the FLAG and HA epitopes were detected by immunofluorescence and confocal microscopy. In the vehicle-treated macrophages, the FLAG and HA epitopes were colocalized at the plasma membrane (Figure 5I). However, after incubation with LGMN, only the HA epitope was detected at the plasma membrane, indicating that LGMN cleaved PAR2 and removed its extracellular FLAG epitope (Figure 5I).

LGMN Deficiency Induces MHC-II^high CCR2+ and MHC-II^low CCR2+ Infiltration After MI

First, we examined cardiac macrophages and observed no overt difference between WT and $Lgmn^{-/-}$ mice (Figure S6A). Next, we used flow cytometry to evaluate the infiltration of cardiac neutrophils and macrophages/monocytes in the $Lgmn$ KO and WT mice after MI. The $Lgmn$ KO mice exhibited significantly more infiltration of Ly-6C+ monocytes and neutrophils at day 5 after MI compared with the WT mice (Figure S6B). In addition, the $Lgmn$ KO mice showed an increased infiltration of MHC-II^high CCR2+ macrophages and an enhanced recruitment of MHC-II^low CCR2+ monocytes at day 5 after MI compared with the WT mice, suggesting that LGMN deficiency resulted in prolonged inflammation and that LGMN-dependent phagocytosis was responsible for inflammation resolution (Figure S6C). However, LGMN deficiency had no significant effect on proliferation of macrophages as determined with BrdU (Figure S6D). Gene expression analyses of the anti-inflammatory mediators interleukin-10 and transforming growth factor-β (Figure S6E) and proinflammatory mediators interleukin-1β, tumor necrosis factor-α, interleukin-6, and interferon-γ (Figure S6F) confirmed delayed inflammation resolution in the $Lgmn$ KO mice after MI compared with the WT mice. Taken together, these findings indicate that LGMN deficiency impaired post-MI inflammation resolution.

Depletion of Lgmn in Resident Cardiac Macrophages Exacerbates Cardiac Function After MI

Next, we used Lgmn^F/F×Cx3cr1^CreER mice to selectively deplete Lgmn in resident cardiac macrophages.[7] To test the functional role of Lgmn in resident macrophages after MI, we fed 3-week-old Lgmn^F/F×Cx3cr1^CreER mice tamoxifen chow diet for 10 days and then discontinued it for 6 weeks. We found that the tamoxifen-treated Lgmn^F/F×Cx3cr1^CreER mice displayed deteriorated cardiac function 14 days after MI compared with Lgmn^F/F×Cx3cr1^CreER mice (Figure 6A and 6B). Furthermore, the infarctions were significantly larger in the tamoxifen-treated Lgmn^F/F×Cx3cr1^CreER mice than in the control Lgmn^F/F×Cx3cr1^CreER mice (Figure 6C). The tamoxifen-treated Lgmn^F/F×Cx3cr1^CreER mice also exhibited increased ratios of heart and lung weight to body weight at day 14 after MI compared with the WT mice, indicating compromised cardiac function in these mice (Table S4). TUNEL staining also confirmed increased cardiomyocyte apoptosis in the hearts of the tamoxifen-treated Lgmn^F/F×Cx3cr1^CreER mice after MI (Figure 6D). The colocalization of cardiomyocyte marker cardiac troponin I and CD68+ macrophages was significantly decreased in the tamoxifen-treated Lgmn^F/F×Cx3cr1^CreER mice at day 7 after MI (Figure 6E). Lyve1 was highly expressed within MHC-II^low CCR2− resident cardiac macrophages and could be used to identify resident cardiac macrophages.[7,17] Next, we crossed the Lgmn^F/F mice with Lyve1^Cre/GFP mice to specifically deplete LGMN in MHC-II^low CCR2− resident cardiac macrophages. As expected, the Lgmn^F/F×Lyve1^Cre/GFP mice exhibited exacerbated effects of MI (Figure S7 and Table S5).

Lgmn Overexpression in Cardiac Macrophages Improves Cardiac Function in Mice After MI

To investigate the beneficial function of LGMN during cardiac remodeling in vivo, $Lgmn$ was transiently expressed using an adenoviral vector (adLgmn; Figure S8A) in the $Lgmn$ KO mice after MI. To verify transfection efficiency and specificity, Lgmn expression was examined by immunofluorescence staining and Western blotting. As shown in Figure S8B, Lgmn expression was detected mainly in macrophages of $Lgmn$ KO mice with $Lgmn$ overexpression (adLgmn-MI). Furthermore, Western blotting assay demonstrated strikingly increased levels of Lgmn protein in adLgmn-MI compared with $Lgmn$ KO mice without $Lgmn$ overexpression (adnull-MI; Figure S8C). There were no significant differences in the body weight measurements between the adLgmn-MI and adnull-MI mice throughout the entire study period (Table S6). However, $Lgmn$ overexpression significantly improved cardiac function at days 7 and 14 after MI (Figure 7A and 7B). In addition, the infarctions of the adLgmn-MI mice were significantly smaller than those of the adnull-MI mice (Figure 7C). The adLgmn-MI mice also exhibited decreased ratios of heart and lung weight to body weight on day 14 after MI compared with adnull-MI mice, indicating improved cardiac function (Table S5). Furthermore, TUNEL staining confirmed decreased
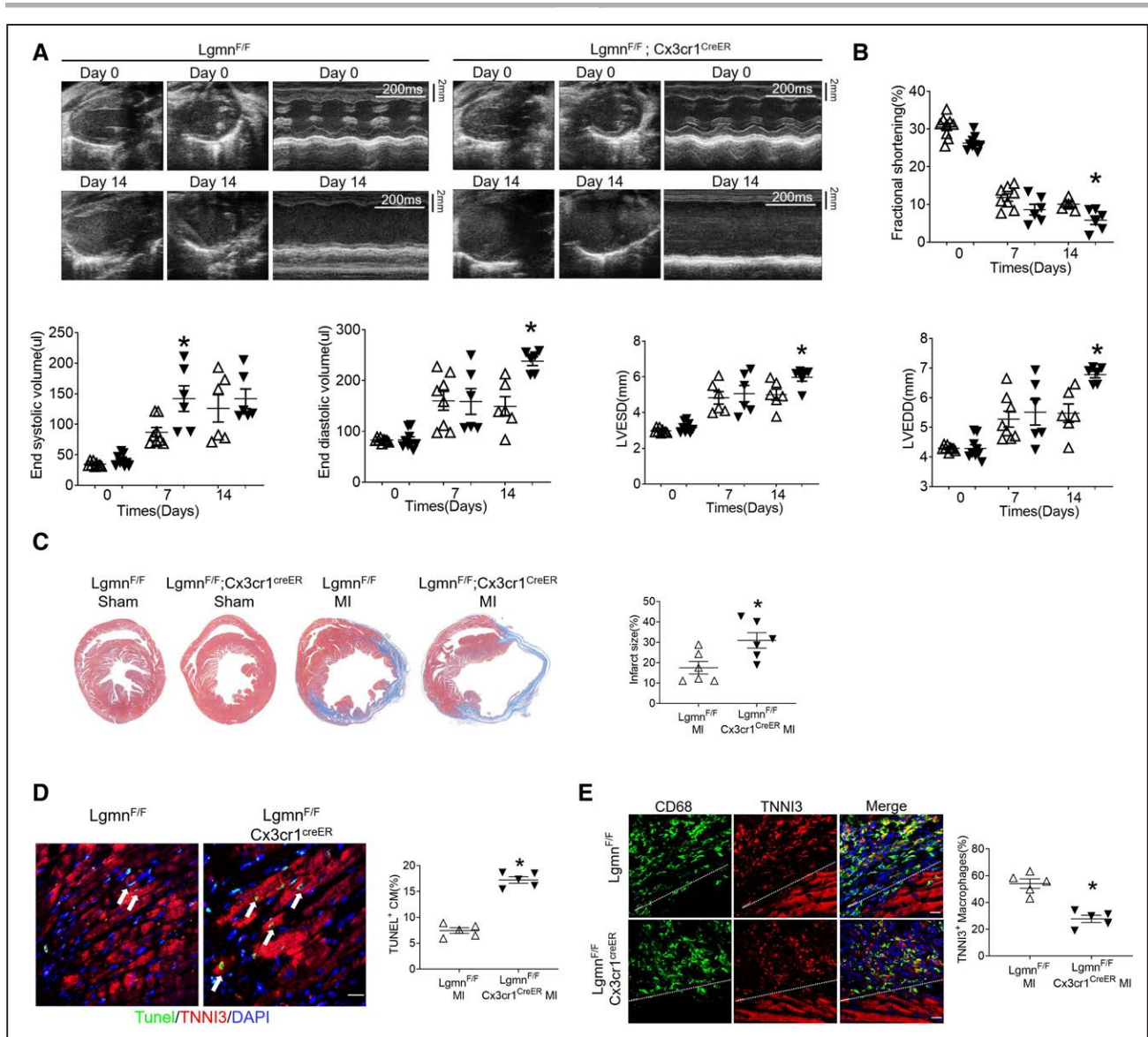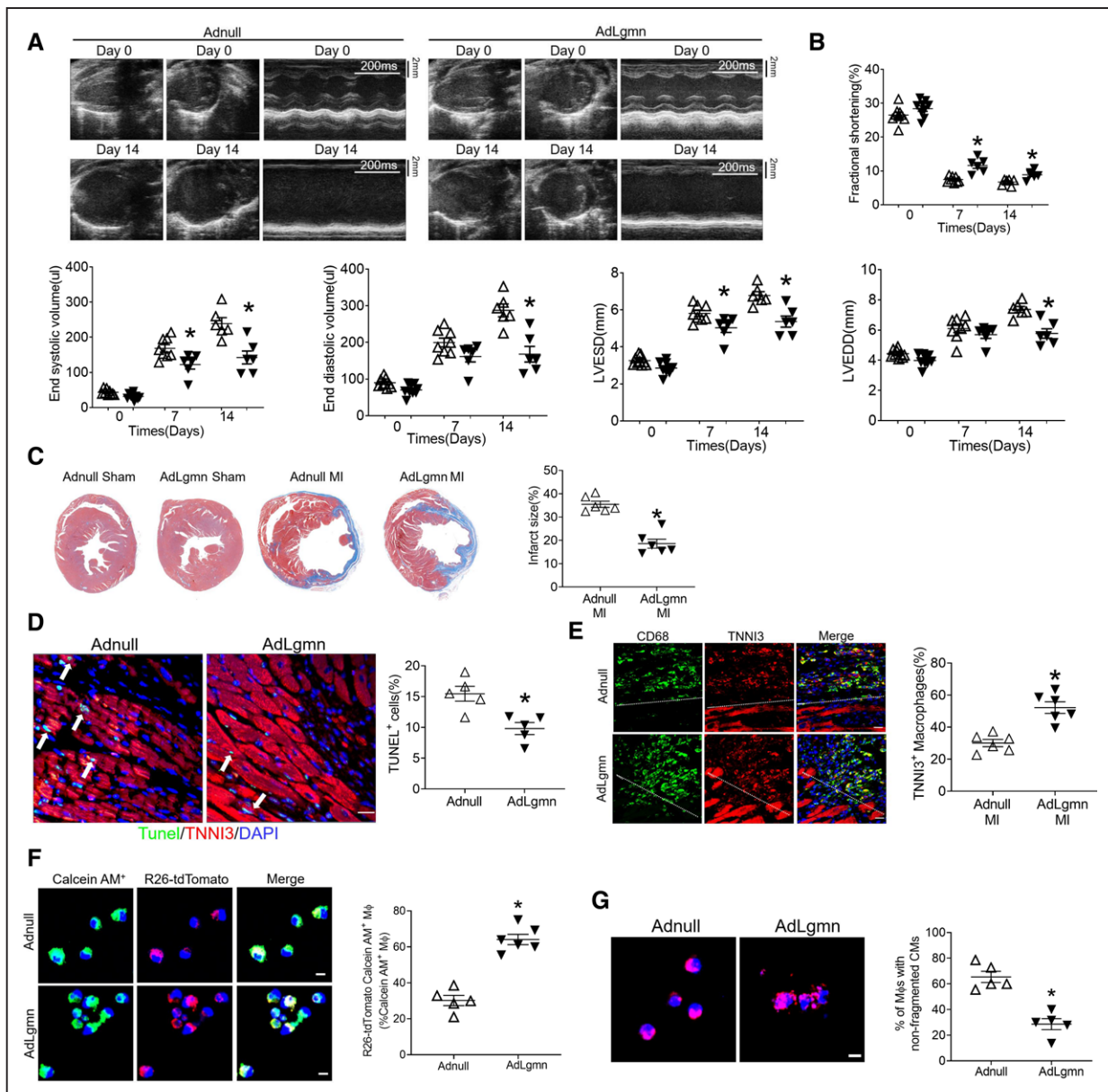
Figure 6. Cardiac function comparison between *Lgmn*^{F/F} and *Lgmn*^{F/F}×Cx3cr1^{CreER} mice after MI.

A and **B**, Representative parasternal long-axis views, short-axis views, and M-mode images. Echocardiographic analysis of left ventricular end-systolic volume (LVESV), left ventricular end-diastolic volume (LVEDV), fractional shortening (FS), left ventricular end-systolic diameter (LVESD), and left ventricular end-diastolic diameter (LVEDD) on days 0, 7, and 14 after the myocardial infarction (MI) or sham operation in *Lgmn*^{F/F} and *Lgmn*^{F/F}×Cx3cr1^{CreER} mice (n=6–9; *P<0.05 by 2-way repeated-measures ANOVA). **C**, Representative Masson trichrome staining of cardiac tissue obtained from *Lgmn*^{F/F} and *Lgmn*^{F/F}×Cx3cr1^{CreER} mice on day 14 after MI or sham operation. Quantitative analysis of infarct size on day 14 after MI in *Lgmn*^{F/F} and *Lgmn*^{F/F}×Cx3cr1^{CreER} mice (n=6; *P<0.05 vs *Lgmn*^{F/F} MI by Mann-Whitney *U* test). **D**, Representative photomicrographs of terminal deoxynucleotidyl transferase dUTP nick-end labeling (TUNEL) and nuclear DAPI staining of cardiomyocyte marker cardiac troponin I (TNNI3)–positive cardiomyocytes obtained from *Lgmn*^{F/F} and *Lgmn*^{F/F}×Cx3cr1^{CreER} mice on day 5 after MI. White arrows point out TUNEL-positive (green) cardiomyocyte (red) nuclei (blue; scale bar, 20 μm). Percentage of TUNEL-positive cardiomyocytes after MI, compared between *Lgmn*^{F/F} and *Lgmn*^{F/F}×Cx3cr1^{CreER} mice (n=5; *P<0.05 vs *Lgmn*^{F/F} MI by Mann-Whitney *U* test). **E**, Immunohistochemistry shows colocalization of CD68+ macrophages with TNNI3+ cardiomyocytes (yellow). Scale bar, 20 μm. Analysis of internalization of cardiomyocyte-derived proteins in macrophages. Macrophages that stain positive for cardiomyocyte TNNI3 are scored as having internalized cardiomyocyte-derived proteins (n=5; *P<0.05 vs *Lgmn*^{F/F} MI by Mann-Whitney *U* test). See Table S7 for statistical details. Lgmn indicates legumain.

cardiomyocyte apoptosis in the hearts of the adLgmn-MI mice after MI in the border area (Figure 7D). The adLgmn-MI mice also exhibited a significant increase in the colocalization of cardiomyocyte marker cardiac troponin I and CD68+ macrophages at day 7 after MI (Figure 7E), indicating improved efferocytosis in these mice. To further explore whether Lgmn-overexpression

on *Lgmn*^{−/−} resident cardiac macrophages would restore macrophage efferocytosis in vitro, we cocultured dying primary adult mouse cardiomyocytes and *Lgmn*^{−/−} resident cardiac macrophages transfected with adnull or adLgmn. AdLgmn resident cardiac macrophages exhibited improved high-burden efferocytosis and an increased phagocytic capacity (Figure 7F and 7G). Taken together,

Figure 7. Cardiac function comparison between adnull and adLgmn mice after MI.

A and **B**, Representative parasternal long-axis views, short-axis views, and M-mode images. Echocardiographic analysis of left ventricular end-systolic volume (LVESV), left ventricular LV end-diastolic volume (LVEDV), fractional shortening (FS), left ventricular end-systolic diameter (LVESD), and left ventricular end-diastolic diameter (LVEDD) on days 0, 7, and 14 after the MI or sham operation in adnull and adLgmn mice (adLgmn: adenoviral vector with Lgmn;adnull: adenoviral vector with null) (n=6–8; *P<0.05 by 2-way repeated-measures ANOVA). **C**, Representative Masson trichrome staining of cardiac tissue obtained from adnull and adLgmn mice on day 14 after MI or sham operation. Quantitative analysis of infarct size on day 14 after MI in adnull and adLgmn mice (n=6; *P<0.05 vs adnull MI by Mann-Whitney U test). **D**, Representative photomicrographs of terminal deoxynucleotidyl transferase dUTP nick-end labeling (TUNEL) and nuclear DAPI staining of cardiomyocyte marker cardiac troponin I (TNNI3)–positive cardiomyocytes obtained from adnull and adLgmn mice on day 5 after MI. White arrows point out TUNEL-positive (green) cardiomyocyte (red) nuclei (blue; scale bar, 20 μm). Percentage of TUNEL-positive cardiomyocytes after MI, compared between adnull and adLgmn mice (n=5; *P<0.05 vs adnull MI by Mann-Whitney U test). **E**, Immunohistochemistry shows colocalization of CD68+ macrophages with TNNI3+ cardiomyocytes (yellow). Scale bar, 20 μm. Analysis of internalization of cardiomyocyte-derived proteins in macrophages. Macrophages that stain positive for cardiomyocyte TNNI3 are scored as having internalized cardiomyocyte-derived proteins (n=6; *P<0.05 vs adnull MI by Mann-Whitney U test). **F**, Lgmn$^{-/-}$ resident cardiac macrophages were transfected with adnull or adLgmn. Adnull or adLgmn macrophages were incubated with calcein AM-labeled cardiomyocytes at a 5:1 cardiomyocyte:macrophage ratio for 45 minutes. Cardiomyocytes were removed and rested for 120 minutes, before macrophages were incubated with R26-tdTomato cardiomyocytes at a 5:1 ratio for 45 minutes. Unengulfed cardiomyocytes were removed, and the percentage of calcein AM+ R26-tdTomato+ macrophages among calcein AM+ macrophages was analyzed by immunofluorescence (n=5–6; *P<0.05 vs adnull by Mann-Whitney U test). **G**, Adnull or adLgmn macrophages were incubated for 45 minutes with R26-tdTomato cardiomyocytes. Unengulfed cardiomyocytes were removed, and macrophages were incubated for 3 hours. Cells were fixed with 2% formaldehyde, and cardiomyocyte fragmentation was quantified as the percentage of macrophages with fragmented R26-tdTomato fluorescence (n=5; *P<0.05 vs adnull by Mann-Whitney U test). Scale bar, 20 mm. See Table S7 for statistical details. Lgmn indicates legumain.

these findings show that the transient overexpression of *Lgmn* significantly improved efferocytosis and cardiac function after MI.

DISCUSSION

The suboptimal clearance of dying cardiomyocytes after MI leads to secondary necrosis, resulting in the further loss of adjacent, nonregenerative cardiomyocytes. Mechanisms that ensure the elimination of apoptotic cardiomyocytes are required to maintain cardiac function and have been the focus of many studies.[18,19] Through the use of a murine model of MI, we report that LGMN deficiency impairs the ability of cardiac macrophages to efficiently clear and degrade apoptotic cardiomyocytes after MI, leading to an accumulation of these apoptotic cells. Impaired efferocytosis also leads to compromised cardiac function and exacerbated cardiac remodeling. Furthermore, LGMN deficiency promotes the accumulation of inflammogenic material and impairs efferocytosis-dependent anti-inflammatory signaling in resident cardiac macrophages.

Significant progress has been made in defining the steps involved in the efferocytosis of apoptotic cells, thus improving our understanding of this complex and evolutionarily conserved process.[20] These steps include the sensing of apoptotic cells through "find me" signals, the recognition of apoptotic cells through "eat me" signals, the activation of cytoskeletal rearrangement signaling pathways required for engulfment, and the regulation of intracellular phagocytic responses for the digestion and processing of the apoptotic cells.[11,20] The efferocytosis of apoptotic cardiomyocytes is critical for protecting the host against unchecked inflammation in the heart. Unengulfed apoptotic cardiomyocytes may leak their intracellular contents, resulting in danger signaling and inflammation.[21] In contrast, phagocytes secrete anti-inflammatory cytokines such as transforming growth factor-β and interleukin-10 on apoptotic cell recognition, thereby dampening or resolving inflammation.[11,20] Proper efferocytosis requires individual cardiac macrophages to ingest multiple apoptotic cardiomyocytes. In this study, we have identified LGMN as an essential lysosomal enzyme during efferocytosis that is needed to prevent the accumulation of apoptotic cardiomyocytes, to guard against the excessive leakage of the contents of the apoptotic cells, and to mediate proper inflammation resolution. The degradation of phagolysosomal cargo is necessary for the efficient uptake of multiple apoptotic cells.[22] If dying cardiomyocytes are not efficiently cleared, they can promote further collateral cell death and incur permanent loss of contractile function. Our data reveal that LGMN deficiency reduces apoptotic cardiomyocyte clearance and therefore exacerbates cardiac damage.

Cardiac resident macrophages have homeostatic and regenerative properties that are important for endocytosis, lysosomal functions, angiogenesis, and regeneration.[7,23] It is known that resident macrophages die within the infarct and survive in the remote area. We showed that MHC-II^{low} CCR2$^-$ macrophages re-emerged within the infarct area at day 5 after MI, but our data are insufficient to determine the origin of these cells that re-emerged within the infarct area after MI. Dick et al[7] demonstrated that these cells might be largely monocyte derived, unlike the prenatally derived resident subset. Future studies are needed to determine the origin of re-emerged MHC-II^{low} CCR2$^-$ macrophages in the infarct zone in our study setting. Recruited macrophages did not express TIMD4, highlighting the ability of using TIMD4 to identify resident macrophages after MI.[7] In this study, we found that Lgmn is expressed mainly in TIMD4$^+$ CCR2$^-$ resident macrophages. Our finding is in line with previous results that under stress conditions such as hypoxia, starvation, and an acidic environment, Lgmn is significantly upregulated and displays significantly higher activity.[24] We showed that resident cardiac macrophages were activated under ischemic environment and were responsible for the increased expression of Lgmn. To explore whether myofibroblasts or endothelial cells also contributed to the increased Lgmn expression after infarction, we found that Lgmn expression was very low in fibroblasts or endothelial cells in the bioGPS databases in human (Figure S9A) and mice (Figure S1B). Results of double-immunofluorescence staining for Lgmn along with endothelial cells marker (CD31) and fibroblast marker (Vimentin) showed that Lgmn expression was very low in endothelial cells and fibroblasts after MI (Figure S9B). In addition, we demonstrated that inducible depletion of Lgmn in resident macrophages using a Cx3cr1-based system and specifically depleted LGMN in resident cardiac macrophages using Lgmn$^{F/F}$×Lyve1$^{Cre/GFP}$ mice impaired macrophage efferocytosis and promoted adverse remodeling, revealing a cardioprotective role of Lgmn in resident cardiac macrophages. LGMN is expressed mainly in MHC-II^{low} CCR2$^-$ macrophages in mice; however, it is expressed predominately in CCR2$^-$ MHC-II^{high} macrophages in humans. Nonetheless, LGMN is indispensable for efficient efferocytosis in these resident macrophages, and no functional differences have been described between mouse CCR2$^-$ MHC-II^{low} and human CCR2$^-$ MHC-II^{high} macrophages beyond antigen presentation.[5] Consistent with mouse CCR2$^-$ MHC-II^{low} macrophages, human CCR2$^-$ MHC-II^{high} macrophages express important resident macrophage markers, including TIMD4 and LYVE1.[7,9] In this study, we have revealed that Lgmn-dependent phagocytosis is required for the maintenance and polarization of resident macrophages and imprints an anti-inflammatory phenotype of cardiac resident macrophages. Impaired efferocytosis after MI almost certainly has multiple causes. A recent study showed that impaired efferocytosis might result from the defective cleavage of the macrophage efferocytosis receptor MerTK in response to inflammation.[18,25] Our

study results hinted that any process that specifically compromises the ability of macrophages to engulf and process multiple apoptotic or dead cells would likely result in unwanted pathological consequences. In addition, macrophages could take up material from leukocytes, endothelial cells, and fibroblasts.[2,25] The present study focused only on cardiomyocytes as the targeted cell type after MI. Primary results showed that the proportion of TUNEL-positive leukocytes, endothelial cells, and fibroblasts was similar between *Lgmn* KO mice and WT mice after MI (Figure S10). Future studies are essential to explore the potential role of Lgmn and specific macrophage subsets in efferocytosis of apoptotic leukocytes, endothelial cells, and fibroblasts. A previous study showed that *Lgmn* KO may aggravate renal dysfunction and fibrosis under the stimulation of unilateral ureteral obstruction.[26] We therefore compared the serum creatinine levels at baseline and after MI between WT and *Lgmn*$^{-/-}$ mice. In the sham-operated group, there was no difference in the creatinine level between WT and Lgmn$^{-/-}$ mice. MI resulted in increased serum creatinine levels in both WT and *Lgmn*$^{-/-}$ mice, and serum creatinine levels after MI tended to be higher in *Lgmn*$^{-/-}$ mice compared with WT mice. In addition, the expression of α-smooth muscle actin and collagen types I/III in kidney tissue was similar between WT and *Lgmn*$^{-/-}$ mice after MI (Figure S11). Future studies are required to determine the extent to which renal dysfunction is involved in the cardiac dysfunction and repair after MI in *Lgmn*$^{-/-}$ mice.

CONCLUSIONS

LGMN deficiency severely impairs macrophage efferocytosis pathways and results in excessive cardiomyocyte death after MI. The proper expression and function of LGMN are critical in response to MI, making the associated pathways particularly tractable for therapeutic intervention. Therefore, strategies to activate LGMN and enhance phagocytosis may be viable approaches for enhancing cardiac protection after MI.

ARTICLE INFORMATION

Affiliations

Department of Cardiology, Zhongshan Hospital, Fudan University, Shanghai Institute of Cardiovascular Diseases, China (D.J., P.B., J.L., A.S., J.G.). Key Laboratory of Viral Heart Diseases, National Health Commission, Shanghai, China (D.J., S.C., P.B., J.L., A.S., J.G.). Key Laboratory of Viral Heart Diseases, Chinese Academy of Medical Sciences, Shanghai, China (D.J., S.C., P.B., J.L., A.S., J.G.). Institutes of Biomedical Sciences, Fudan University, Shanghai, China (S.C., A.S., J.G.). Department of Cardiovascular Surgery, Zhejiang Provincial People's Hospital, People's Hospital of Hangzhou Medical College, China (C.L.).

Sources of Funding

Disclosures

None.

Supplemental Material

Expanded Methods and Materials
Supplemental Material Figures S1–S11
Supplemental Material Tables S1–S7
References 27–33

REFERENCES

1. Bauersachs J. Heart failure drug treatment: the fantastic four. *Eur Heart J.* 2021;42:681–683. doi: 10.1093/eurheartj/ehaa1012
2. Zhang S, Dehn S, DeBerge M, Rhee KJ, Hudson B, Thorp EB. Phagocyte-myocyte interactions and consequences during hypoxic wound healing. *Cell Immunol.* 2014;291:65–73. doi: 10.1016/j.cellimm.2014.04.006
3. Wan E, Yeap XY, Dehn S, Terry R, Novak M, Zhang S, Iwata S, Han X, Homma S, Drosatos K, et al. Enhanced efferocytosis of apoptotic cardiomyocytes through myeloid-epithelial-reproductive tyrosine kinase links acute inflammation resolution to cardiac repair after infarction. *Circ Res.* 2013;113:1004–1012. doi: 10.1161/CIRCRESAHA.113.301198
4. Zhang S, Yeap XY, Grigoryeva L, Dehn S, DeBerge M, Tye M, Rostlund E, Schrijvers D, Zhang ZJ, Sumagin R, et al. Cardiomyocytes induce macrophage receptor shedding to suppress phagocytosis. *J Mol Cell Cardiol.* 2015;87:171–179. doi: 10.1016/j.yjmcc.2015.08.009
5. Epelman S, Lavine KJ, Beaudin AE, Sojka DK, Carrero JA, Calderon B, Brija T, Gautier EL, Ivanov S, Satpathy AT, et al. Embryonic and adult-derived resident cardiac macrophages are maintained through distinct mechanisms at steady state and during inflammation. *Immunity.* 2014;40:91–104. doi: 10.1016/j.immuni.2013.11.019
6. Vandivier RW, Henson PM, Douglas IS. Burying the dead: the impact of failed apoptotic cell removal (efferocytosis) on chronic inflammatory lung disease. *Chest.* 2006;129:1673–1682. doi: 10.1378/chest.129.6.1673
7. Dick SA, Macklin JA, Nejat S, Momen A, Clemente-Casares X, Althagafi MG, Chen JM, Kantores C, Hosseinzadeh S, Aronoff L, et al. Self-renewing resident cardiac macrophages limit adverse remodeling following myocardial infarction. *Nature Immunol.* 2019;20:664–664.
8. Yan X, Zhang H, Fan Q, Hu J, Tao R, Chen Q, Iwakura Y, Shen W, Lu L, Zhang Q, et al. Dectin-2 deficiency modulates Th1 differentiation and improves wound healing after myocardial infarction. *Circ Res.* 2017;120:1116–1129. doi: 10.1161/CIRCRESAHA.116.310260
9. Bajpai G, Schneider C, Wong N, Bredemeyer A, Hulsmans M, Nahrendorf M, Epelman S, Kreisel D, Liu Y, Itoh A, et al. The human heart contains distinct macrophage subsets with divergent origins and functions. *Nat Med.* 2018;24:1234–1245. doi: 10.1038/s41591-018-0059-x
10. Fan Q, Tao R, Zhang H, Xie H, Lu L, Wang T, Su M, Hu J, Zhang Q, Chen Q, et al. Dectin-1 contributes to myocardial ischemia/reperfusion injury by regulating macrophage polarization and neutrophil infiltration. *Circulation.* 2019;139:663–678. doi: 10.1161/CIRCULATIONAHA.118.036044
11. Hochreiter-Hufford A, Ravichandran KS. Clearing the dead: apoptotic cell sensing, recognition, engulfment, and digestion. *Cold Spring Harb Perspect Biol.* 2013;5:a008748. doi: 10.1101/cshperspect.a008748
12. Martinez J, Almendinger J, Oberst A, Ness R, Dillon CP, Fitzgerald P, Hengartner MO, Green DR. Microtubule-associated protein 1 light chain 3 alpha (LC3)-associated phagocytosis is required for the efficient clearance of dead cells. *Proc Natl Acad Sci USA.* 2011;108:17396–17401. doi: 10.1073/pnas.1113421108
13. Martinez J, Cunha LD, Park S, Yang M, Lu Q, Orchard R, Li QZ, Yan M, Janke L, Guy C, et al. Noncanonical autophagy inhibits the autoinflammatory, lupus-like response to dying cells. *Nature.* 2016;533:115–119. doi: 10.1038/nature17950
14. Cuttell L, Vaughan A, Silva E, Escaron CJ, Lavine M, Van Goethem E, Eid JP, Quirin M, Franc NC. Undertaker, a Drosophila junctophilin, links Draper-mediated phagocytosis and calcium homeostasis. *Cell.* 2008;135:524–534. doi: 10.1016/j.cell.2008.08.033

15. Gronski MA, Kinchen JM, Juncadella IJ, Franc NC, Ravichandran KS. An essential role for calcium flux in phagocytes for apoptotic cell engulfment and the anti-inflammatory response. *Cell Death Differ.* 2009;16:1323–1331. doi: 10.1038/cdd.2009.55

16. Tu NH, Jensen DD, Anderson BM, Chen E, Jimenez-Vargas NN, Scheff NN, Inoue K, Tran HD, Dolan JC, Meek TA, et al. Legumain induces oral cancer pain by biased agonism of protease-activated receptor-2. *J Neurosci.* 2021;41:193–210. doi: 10.1523/JNEUROSCI.1211-20.2020

17. Mass E, Ballesteros I, Farlik M, Halbritter F, Günther P, Crozet L, Jacome-Galarza CE, Händler K, Klughammer J, Kobayashi Y, et al. Specification of tissue-resident macrophages during organogenesis. *Science.* 2016;353:aaf4238. doi: 10.1126/science.aaf4238

18. Zhang S, Yeap XY, Grigoryeva L, Dehn S, DeBerge M, Tye M, Rostlund E, Schrijvers D, Zhang ZJ, Sumagin R, et al. Cardiomyocytes induce macrophage receptor shedding to suppress phagocytosis. *J Mol Cell Cardiol.* 2015;87:171–179. doi: 10.1016/j.yjmcc.2015.08.009

19. DeBerge M, Yeap XY, Dehn S, Zhang S, Grigoryeva L, Misener S, Procissi D, Zhou X, Lee DC, Muller WA, et al. MerTK cleavage on resident cardiac macrophages compromises repair after myocardial ischemia reperfusion injury. *Circ Res.* 2017;121:930–940. doi: 10.1161/CIRCRESAHA.117.311327

20. Elliott MR, Ravichandran KS. Clearance of apoptotic cells: implications in health and disease. *J Cell Biol.* 2010;189:1059–1070. doi: 10.1083/jcb.201004096

21. Frangogiannis NG. Pathophysiology of myocardial infarction. *Compr Physiol.* 2015;5:1841–1875. doi: 10.1002/cphy.c150006

22. Wang Y, Subramanian M, Yurdagul A Jr, Barbosa-Lorenzi VC, Cai B, de Juan-Sanz J, Ryan TA, Nomura M, Maxfield FR, Tabas I. Mitochondrial fission promotes the continued clearance of apoptotic cells by macrophages. *Cell.* 2017;171:331–345.e22. doi: 10.1016/j.cell.2017.08.041

23. Jia D, Jiang H, Weng X, Wu J, Bai P, Yang W, Wang Z, Hu K, Sun A, Ge J. Interleukin-35 promotes macrophage survival and improves wound healing after myocardial infarction in mice. *Circ Res.* 2019;124:1323–1336. doi: 10.1161/CIRCRESAHA.118.314569

24. Bai P, Lyu L, Yu T, Zuo C, Fu J, He Y, Wan Q, Wan N, Jia D, Lyu A. Macrophage-derived Legumain promotes pulmonary hypertension by activating the MMP (matrix metalloproteinase)-2/TGF (transforming growth factor)-β1 signaling. *Arterioscler Thromb Vasc Biol.* 2019;39:e130–e145. doi: 10.1161/ATVBAHA.118.312254

25. Nicolás-Ávila JA, Lechuga-Vieco AV, Esteban-Martínez L, Sánchez-Díaz M, Díaz-García E, Santiago DJ, Rubio-Ponce A, Li JL, Balachander A, Quintana JA, et al. A network of macrophages supports mitochondrial homeostasis in the heart. *Cell.* 2020;183:94–109.e23. doi: 10.1016/j.cell.2020.08.031

26. Wang D, Xiong M, Chen C, Du L, Liu Z, Shi Y, Zhang M, Gong J, Song X, Xiang R, et al. Legumain, an asparaginyl endopeptidase, mediates the effect of M2 macrophages on attenuating renal interstitial fibrosis in obstructive nephropathy. *Kidney Int.* 2018;94:91–101. doi: 10.1016/j.kint.2017.12.025

27. Gao E, Lei YH, Shang X, Huang ZM, Zuo L, Boucher M, Fan Q, Chuprun JK, Ma XL, Koch WJ. A novel and efficient model of coronary artery ligation and myocardial infarction in the mouse. *Circ Res.* 2010;107:1445–1453. doi: 10.1161/CIRCRESAHA.110.223925

28. Mathiyalagan P, Adamiak M, Mayourian J, Sassi Y, Liang Y, Agarwal N, Jha D, Zhang S, Kohlbrenner E, Chepurko E, et al. FTO-dependent N6-methyladenosine regulates cardiac function during remodeling and repair. *Circulation.* 2019;139:518–532. doi: 10.1161/CIRCULATIONAHA.118.033794

29. Ackers-Johnson M, Li PY, Holmes AP, O'Brien SM, Pavlovic D, Foo RS. A simplified, Langendorff-free method for concomitant isolation of viable cardiac myocytes and nonmyocytes from the adult mouse heart. *Circ Res.* 2016;119:909–920. doi: 10.1161/CIRCRESAHA.116.309202

30. Kim D, Langmead B, Salzberg SL. HISAT: a fast spliced aligner with low memory requirements. *Nat Methods.* 2015;12:357–360. doi: 10.1038/nmeth.3317

31. Pertea M, Pertea GM, Antonescu CM, Chang TC, Mendell JT, Salzberg SL. StringTie enables improved reconstruction of a transcriptome from RNA-seq reads. *Nat Biotechnol.* 2015;33:290–295. doi: 10.1038/nbt.3122

32. Robinson MD, McCarthy DJ, Smyth GK. edgeR: a bioconductor package for differential expression analysis of digital gene expression data. *Bioinformatics.* 2010;26:139–140. doi: 10.1093/bioinformatics/btp616

33. Zuo S, Kong D, Wang C, Liu J, Wang Y, Wan Q, Yan S, Zhang J, Tang J, Zhang Q, et al. CRTH2 promotes endoplasmic reticulum stress-induced cardiomyocyte apoptosis through m-calpain. *EMBO Mol Med.* 2018;10:e8237. doi: 10.15252/emmm.201708237